REMARKS

Initially, Applicants notice that the Examiner did not attach to the Office Action an initialed copy of Form 1449, and respectfully request that this form be initialed and returned.

Applicants have corrected typographical errors in the Specification and revised the abstract. Support for the revision to the abstract can be found at page 1, line 19 to page 2, line 18 of the Specification. No new matter has been introduced by the amendments.

Claims 1-21 are now pending. Reconsideration of the application, as amended, is requested in view of the remarks below.

The Examiner concluded that claims 12-14 and 21 are allowable if rewritten in independent form. See the Office Action, page 4, lines 8-10.

Claims 1-11 and 15-20, on the other hand, were rejected under 35 U.S.C. 103(a) as being obvious over Hironaka et al., U.S. Patent No. 5,336,546 ("Hironaka")[1]. See the Office Action, page 3, lines 1-2. Applicants respectfully traverse the ground for rejection as follows.

Claim 1 is drawn to compounds of the following formula:

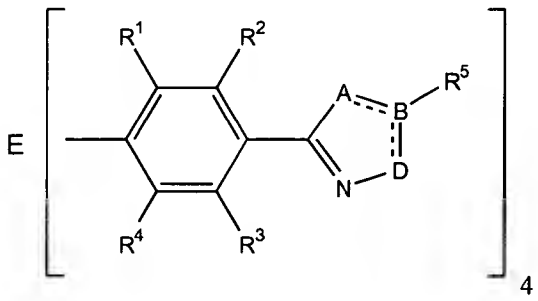

Each variable is defined in claim 1. The compounds closest to the compounds described in Hironaka are methane substituted with four oxadiazole-containing moieties, and will be referred to as "oxadiazole tetramer." Formulae of exemplary oxadiazole tetramers can be found at pages 4-5 of the Specification.

Hironaka discloses oxadiazole compounds that include two oxadiazole moieties. In other words, it discloses oxadiazole dimers. The Examiner pointed out that "Hironaka discloses electroluminescence device wherein an oxadiazole compound is interposed between two electrodes ..." and concluded that "it would have been obvious to one of ordinary skill in the art

[1] The Examiner erroneously stated that claims 1-21, instead of claims 1-11 and 15-20, were rejected on this ground.

to use an oxadiazole tetramer in order to have a light-emitting layer that has greater luminescence performance..." See the Office Action, page 3, lines 3-4 and page 4, lines 4-7.

Ex parte Bywater and Coleman, 83 USPQ 4 (POBI, 1949) is a case in point. It involved substituted hydantoins that differed from the prior art compounds in that the claimed compounds had two, rather than one, thienyl groups substituted on the same ring carbon. It was held that the prior art compounds do not render the claimed compound obvious:

> The compounds defined by the appealed claims are not homologs or isomers of any of the compounds disclosed in the Spurlock reference. We do not believe that the examiner has shown that it would be obvious from the reference to substitute a second thienyl group for the hydrocarbon radical represented by R in the structural formula given in the Spurlock reference. No suggestion for such substitution comes from the reference (emphasis added).

The relevant compounds covered by claim 1 are methane substituted with four oxadiazole-containing moieties, while the closest compounds disclosed in Hironaka are methane substituted with two oxadiazole-containing moieties. The claimed compounds are not homologs or isomers of those disclosed in Hironaka. Further, Hironaka does not suggest substituting methane with four oxadiazole-containing moieties as required by claim 1. Thus, in light of the *Bywater* holding, claim 1 is not rendered obvious by Hironaka. In other words, the Examiner has failed to establish a *prima facie* case of obviousness against claim 1.

Even if a *prima facie* case of obviousness has been made (which Applicants do not concede), it can be successfully rebutted by a showing of unexpected results.

More specifically, an oxadiazole tetramer covered by claim 1 (e.g., compound p-TPAOXD, see page 5 of the Specification) has a much higher glass transition temperature (T_g) than those of oxadiazole dimers (e.g., compounds EM2-EM4, see Tamoto et al., Chem. Mater., (1997) 9:1077-1085, a copy of which is attached hereto as "Exhibit A"). Compound p-TPAOXD is methane substituted with four diphenylaminophenyl-2-oxadiazolylphenyl groups. Compounds EM2-EM4 are benzene substituted with two diphenylaminophenyl-2-oxadiazolyl groups in o-, m-, or p- position. Referring to Table 2 of the Specification and Table 1 of Exhibit A, p-TPAOXD has a T_g of 187°C, which is 65-87°C higher than those of compounds EM2-EM4, i.e.,

99.3-122.3°C[2]. Applicants submit that these unexpected results have successfully rebutted the alleged *prima facie* case of obviousness against claim 1.

Thus, claim 1, as well as claims 2-11 dependent from claim 1, is not rendered obvious by Hironaka.

Claim 15 is drawn to an electroluminescence device containing a compound of claim 1. For the reasons set for above, claim 15 is also not rendered obvious by Hironaka. Neither are claims 16-20 dependent from claim 15.

CONCLUSION

Applicants submit that the ground for rejection asserted by the Examiner has been overcome, and that claims 1-21, as pending, define subject matter that is nonobvious. On this basis, it is submitted that all claims are now in condition for allowance, an action of which is requested.

[2] Note that electroluminescence devices made of compounds with higher T_gs are more stable than those made of compounds with lower T_gs. See the Specification, page 6, lines 19-21.

Articles

Electroluminescence of 1,3,4-Oxadiazole and Triphenylamine-Containing Molecules as an Emitter in Organic Multilayer Light Emitting Diodes

Nozomu Tamoto, Chihaya Adachi,*,† and Kazukiyo Nagai‡

Chemical Products R&D Center, Ricoh Co. Ltd., 146-1 Nishisawada, Numazu-shi, Shizuoka 410, Japan

Received July 22, 1996. Revised Manuscript Received January 13, 1997®

We synthesized five new emitter molecules having an oxadiazole group as an electron transport unit and a triphenylamine group as a hole transport unit. We investigated the electroluminescent (EL) properties of these molecules as an emitter layer. The deposited films of all compounds were found to be amorphous and showed strong blue-green fluorescence, ranging from 450 to 490 nm. With the best device using these emitters, the maximum luminance exceeded 19 000 cd/m^2. We observed that external EL quantum efficiencies (ϕ_{EL}) were drastically influenced by combinations of hole-transport materials. Formation of exciplexes between the emitters and hole-transport materials was found to greatly influence ϕ_{EL}. We observed that the hole-transport layers (HTLs) having a low ionization potential (Ip) value tended to form exciplexes with the emitter layers, resulting in a low ϕ_{EL}. On the other hand, the HTLs having a large Ip formed no exciplexes with emitter layers and showed a high ϕ_{EL}. In the best device, a ϕ_{EL}~4% was obtained. Furthermore, we also studied the optimum EL cell structures using the bipolar emitters. We observed that a double hetero (DH) structure was the best device structure and could achieve an external energy conversion efficiency (ϕ_{energy}) of 3.75 lm/W at a current density of 10 mA/cm^2. This is an excellent value among the organic EL devices previously reported. In addition, the durabilities of the EL devices were also measured at constant current density. Performances of the EL device durabilities were quite inferior with these emitter materials. The time for the luminance to decay to half of the initial luminance was below 1 h.

Introduction

In 1990, it was found that 2-(4-biphenylyl)-5-(4-*tert*-butylphenyl)-1,3,4-oxadiazole (PBD) functions very well as an excellent electron-transport material (ETM) in organic multilayer electroluminescent (EL) diodes.[1,2] From the standpoint of confinement of charge carriers and molecular excitons, the PBD electron-transport layer (ETL) showed marked ability, in analogy with a triphenylamine hole-transport layer (HTL). After this report, many researchers began to use various kinds of oxadiazole derivatives and revealed that 1,3,4-oxadiazole rings function well as an electron-transport moiety.[3−10] In addition to the use of various derivatives of oxadiazole molecules for obtaining high EL performance, in recent studies in the field of polymer light-emitting diodes, significant improvement of EL quantum efficiency was also observed by incorporation of an oxadiazole layer, occasionally polymerized oxadiazoles, between an emitter layer (EML) and a cathode.[11−23] Moreover, it was reported that single molecularly doped polymer films containing PBD and its derivatives

† Present address: Department of Functional Polymer Science, Faculty of Textile Science and Technology, Shinshu University, Ueda 386, Japan. adachic@giptc.shinshu-u.ac.jp.

‡ k-nagai@nts.ricoh.co.jp.

® Abstract published in *Advance ACS Abstracts*, April 1, 1997.

(1) Adachi, C.; Tsutsui, T.; Saito, S. *Appl. Phys. Lett.* **1990**, *56*, 799.
(2) Adachi, C.; Tsutsui, T.; Saito, S. *Appl. Phys. Lett.* **1990**, *57*, 513.
(3) Kido, J.; Nagai, K.; Okamoto, Y.; Skotheim, T. *Chem. Lett.* **1991**, 1267.
(4) Utsuki, K.; Takano, S. *J. Electrochem. Soc.* **1992**, *139*, 3610.
(5) Ohmori, Y.; Uchida, M.; Morishima, C.; Fujii, A.; Yoshino, K. *Jpn. J. Appl. Phys.* **1993**, *32*, L1663.
(6) Takada, N.; Tsutsui, T.; Saito, S. *Appl. Phys. Lett.* **1993**, *63*, 2032.
(7) Kido, J.; Hayase, H.; Hongawa, K.; Nagai, K.; Okuyama, K. *Appl. Phys. Lett.* **1994**, *65*, 2124.
(8) Era, M.; Morimoto, S.; Tsutsui, T.; Salto, S. *Appl. Phys. Lett.* **1994**, *65*, 676.
(9) Era, M.; Tsutsui, T.; Saito, S. *Appl. Phys. Lett.* **1995**, *67*, 2436.
(10) Kraft, A. *Chem. Commun.* **1996**, 77.
(11) Higashi, H.; Hosokawa, C.; Tokailin, H. *Nippon kagaku-kaishi* **1992**, *10*, 1162 [in Japanese].
(12) Hosokawa, C.; Kawasaki, N.; Sakamoto, S.; Kusumoto, T. *Appl. Phys. Lett.* **1992**, *61*, 2503.
(13) Brown, A. R.; Bradley, D. D. C.; Burroughes, J. H.; Friend, R. H.; Greenham, N. C.; Burn, P. L.; Holmes, A. B.; Kraft, A. *Appl. Phys. Lett.* **1992**, *61*, 2793.
(14) Friend, R.; Bradley, D.; Holmes, A. *Phys. World* **1992**, *5*, 842.
(15) Holemes, A. B.; Bradley, D. D. C.; Brown, A. R.; Burn, P. L.; Burroughes, J. H.; Friend, R. H.; Greenham, N. C.; Gymer, R. W.; Halliday, D. A.; Jackson, R. W.; Kraft, A.; Martens, J. H. F.; Pichler, K.; Samuel, I. D. W. *Synth. Met.* **1993**, *55−57*, 4031.
(16) Berggren, M.; Gustafsson, G.; Inganäs, O.; Anderson, M. R.; Hjertberg, T.; Wennerström, O. *J. Appl. Phys.* **1994**, *76*, 7530.
(17) Li, X.-C.; Yang, Y. *Chem. Mater.* **1995**, *7*, 1568.
(18) Spencer, G. C.; Cacialli, F.; Grüner, J.; Friend, R. H. *J. Chem. Soc., Chem. Commun.* **1995**, 2211.
(19) Pei, Q.; Yang, Y. *Chem. Mater.* **1995**, *7*, 1568.
(20) Pei, Q.; Yang, Y. *Adv. Mater.* **1995**, *7*, 559.

S0897-4756(96)00391-2 CCC: $14.00

showed sufficient importance as doped electron-transport molecules.[24-31]

Besides the use of oxadiazole molecules as an ETM, Hamada et al. synthesized interesting materials which were composed of oxadiazole and dimethylamine groups.[32-34] They showed that these materials were useful for an EML instead of an ETL. Because the dimethylamine group has hole-transport ability, the molecules have a bipolar transport character and thus offered good recombination sites for hole and electron charge carriers. Furthermore, in our study, we developed these emitter materials. We synthesized five new emitters having triphenylamine groups instead of dimethylamine groups as a hole-transport moiety. It is well-known that molecules having a dimethylamine group show low hole mobility below 10^{-7} cm^2/V s. Thus, they have an inferior hole-transport character.[35] On the other hand, triphenylamine groups are known to possess a superior hole-transport mobility.[36,37] The mobilities exceeded 10^{-5} cm^2/V s. When we incorporate these units into the molecular structure of emitters, we can then expect improved bipolar character and improved EL characteristics. We expect high carrier mobilities to contribute to a reduction of the driving voltage, resulting in an increase in energy conversion efficiency. We presume that it is requisite to provide a bipolar character to emitter materials, because the EL of organic materials occurs from a recombination of an anion radical and a cation radical of emitter molecules, resulting in formation of a molecular exciton and successive radiative decay of an exciton. Thus, in view of EL processes, emitters must possess essentially a bipolar nature. If emitter molecules have a unipolar characteristic, excited states have to be produced at the interface of the emitter/carrier transport layers and result in exciplex emission, emission from charge-transfer complexes, and, so on.

In another aspect, providing a bipolar character to an emitter molecule is advantageous for relaxation of exciplex formation between emitter and carrier transport layers. Previously, we have encountered many

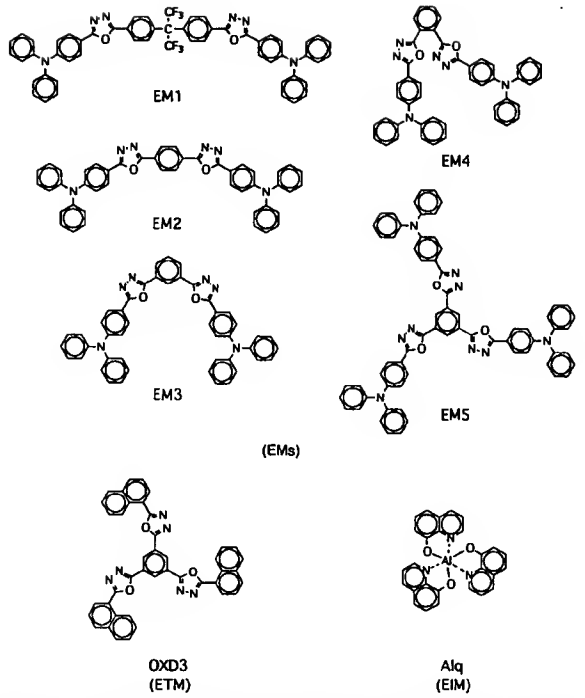

Figure 1. Chemical structures of five bipolar emitters (EM1–EM5), an electron-transport material (ETM), and an electron injection material (E2M) used in this study.

exciplex formations at the interface of organic layers in various material combinations. For example, the combination of a PBD and an *N,N*-diphenyl-*N,N*-bis(3-methylphenyl)-[1,1′-biphenyl]-4,4′-diamine (TPD) forms an exciplex, resulting in a broad red-shift in the EL emission spectrum. Even tris(8-quinolinolato)aluminum (Alq) sometimes forms an exciplex with triphenylamines having low ionization potential (Ip). In a survey of material combinations, we were certain to encounter these problems. In organic multilayer devices, the interaction of adjoining organic layers is very significant. Thus, providing a bipolar character to emitters is surely expected to relieve exciplex formation. With our materials, we observed systematic interaction between various hole-transport and emitter materials. It was revealed that the selection of hole-transport materials greatly influenced the EL quantum efficiency (ϕ_{EL}).[38] We will discuss the detailed experimental results of exciplex formation between these materials.

Furthermore, we also studied the optimum EL cell structures using the emitter materials. As shown in Figure 3, we constructed five kinds of EL cell structures and compared them. With our best device, a large energy conversion efficiency (ϕ_{energy})[38] was obtained with a double hetero (DH) structure. Moreover, the dependence of ϕ_{EL} on EL cell structures gave us significant information on the bipolar nature of emitter layers. We will discuss optimum EL cell structures in connection with the nature of EMLs. Finally, we briefly report on the durabilities of EL devices under continuous dc operation. We observed a considerable rapid decrease of luminance with time.

(21) Buchwald, E.; Meier, M.; Karg, S.; Pösch, P.; Schmidt, H-W.; Strohriegl, P.; Riess, W.; Schwoerer, M. *Adv. Mater.* **1995**, *7*, 839.
(22) Anderson, M. R.; Berggren, M.; Inganäs, O.; Gustafsson, G.; Gustafsson-Carlberg, J. C.; Selse, D.; Hjertberg, T.; Wennerström, O. *Macromolecules* **1995**, *28*, 7525.
(23) Berggren, M.; Inganäs, O.; Gustafsson, G. *Synth. Met.* **1995**, *71*, 2185.
(24) Mori, Y.; Aoyagi, C.; Endo, H.; Hayashi, Y. ; Dozono, T. *Polym. Prepr. Jpn.* **1991**, *40*, 3591.
(25) Mori, Y.; Endo, H.; Hayashi, Y. *Ouyoubitsuri* **1992**, *61*, 1044 [in Japanese].
(26) Lin, C. P.; Tsutsui, T.; Saito, S. *Rep. Prog. Polym. Phys. Jpn.* **1994**, *37*, 431.
(27) Zhang, C.; Höger, S.; Pakbaz, K.; Wudl, F.; Heeger, A. J. *J. Electron. Mater.* **23**, 453.
(28) Zhang, C.; Seggern, H. V.; Kraabel, B.; Schmidt, H.-W.; Heeger, A. J. *Synth. Met.* **1995**, *72*, 185.
(29) Lee, J-K.; Schrock, R. R.; Baigent, D. R.; Friend, R. H. *Macromolecules* **1995**, *28*, 1966.
(30) Fujii, A.; Kawahara, H.; Yoshida, M.; Ohmiri, Y.; Yoshino, K. *J. Phys. D: Appl. Phys.* **1994**, *28*, 2135.
(31) Johnson, G. E.; McGrane, K. M.; Stolka, M. *Pure Appl. Chem.* **1995**, *67*, 175.
(32) Hamada, Y.; Adachi, C.; Tsutsui, T.; Saito, S. *Jpn. J. Appl. Phys.* **1992**, *31*, 1812.
(33) Hamada, Y.; Adachi, C.; Tsutsui, T.; Saito, S. Nippon Kagakukaishi **1991**, *11*, 1540 [in Japanese].
(34) Hamada, Y.; Adachi, C.; Tsutsui, T.; Saito, S. *Optoelectronics* **1992**, *7*, 83.
(35) Takahashi, R.; Kusabayashi, S.; Yokoyama, M. *Denshi-shashin Gakkai-shi* **1986**, *25*, 16 [in Japanese].
(36) Stolka, M.; Yanus, J.; Pai, D. *J. Phys. Chem.* **1984**, *88*, 4707.
(37) Facci, J.; Stolka, M. *Philos. Mag. B* **1986**, *54*, 1.

(38) Here, we define ϕ_{EL} external quantum efficiency; emitted photon/ injected charge carriers. We also define ϕ_{energy} external energy conversion efficiency; emitted photon energy/input energy J(current density) × V(driving voltage).

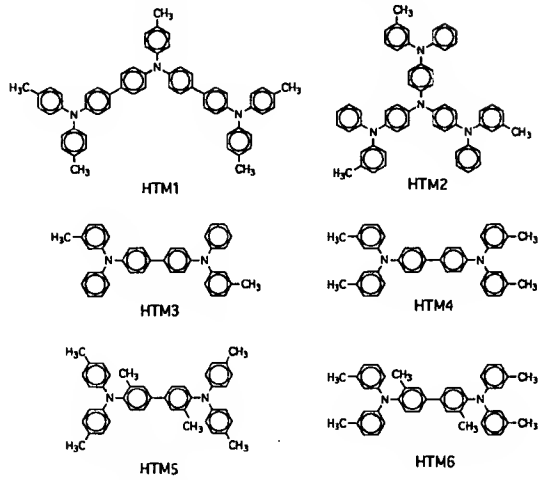

Figure 2. Chemical structures of six hole-transport materials (HTM) used in this study.

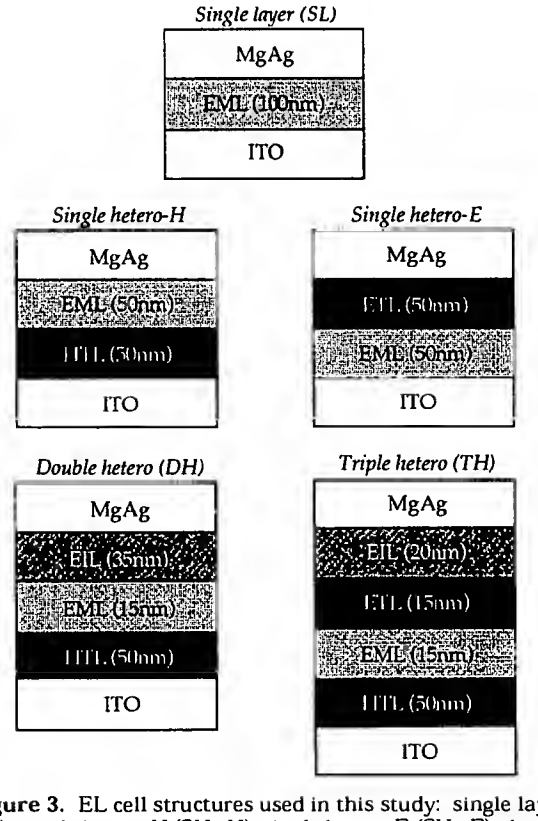

Figure 3. EL cell structures used in this study: single layer (SL), single hetero-H (SH−H), single hetero-E (SH−E), double hetero (DH), and triple hetero (TH).

Experimental Section

1. Organic Materials. Synthesis of oxadiazole derivatives (Schemes 1 and 2): Schemes 1 and 2 show two synthetic routes of oxadiazole derivatives used in this study. Because our previous study showed that the pathway of a tetrazole derivative resulted in a high yield in comparison with the pathway of a hydrazide, we adopted Scheme 1 in the synthesis of the oxadiazole derivatives.[39-42]

4-Cyanotriphenylamine (1): A mixture of *N,N*-diphenylaminobenzaldehyde (15.00 g), hydroxyamine hydrochloride (4.60 g), acetic acid (11.30 g), DMF (40 mL), and pyridine (6.51 g) was stirred and heated at 138 °C for 2.5 h. The product was purified by column chromatography (developing solvent: toluene) and recrystallized from *n*-hexane. Yield 12.66 g (85.2%), mp 125.8−126.5 °C. IR V_{CN}/cm^{-1} 2200.

Scheme 1. Via Tetrazole

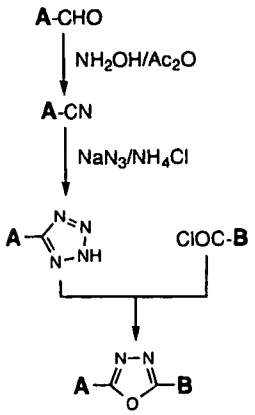

Scheme 2. Via Hydrazide

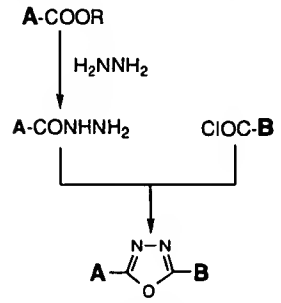

4-Tetrazolyltriphenylamine (2): A mixture of 4-cyanotriphenylamine (**1**, 1.40 g), sodium azide (5.40 g), ammonium chloride (4.44 g), and dry DMF (40 mL) was stirred and heated under reflux for 75 h. The cooled solution was then added to aqueous hydrochloric acid. The precipitate was collected and washed with water. Recrystallization from toluene gave the desired products (2). Yield 12.21 g (91.5%), mp 216.3−217.3 °C. Found: C, 72.91%; H, 4.82%; N, 22.40%. Calcd: C, 72.83%; H, 4.82%; N, 22.35%.

Synthesis of EM1: A mixture of 4-tetrazolyltriphenylamine (2, 1.40 g), 2,2-bis(4-chloroholmylphenyl)hexafluoropropane (0.94 g) and dry pyridine (40 mL) was stirred and heated under reflux for 100 h. After the mixture was cooled, the solvent was evaporated. The crude product was then purified by column chromatography (developing solvent; chloroform:THF = 30:1 v/v) and recrystallized from c-Hex/*n*-Hex. Yield 0.53 g (26.0%), mp 162.0−166.0 °C. Found: C, 71.44%; H, 4.12%; N, 8.88%. Calcd: C, 71.27%; H, 3.91%; N, 9.07%. ^{1}H NMR ($CDCl_3$) δ 7.12−8.16 (m, 36H, aromatic H).

Synthesis of EM2: A mixture of 4-tetrazolyltriphenylamine (2, 3.14 g), *m*-phthaloyl chloride (1.10 g) and dry pyridine (90 mL) was stirred and heated under reflux for 58 h. After cooling, the mixture was poured into water, and the precipitate was collected and washed with water. After the mixture was cooled, the crude product was purified by column chromatography (developing solvent; chloroform:THF = 30:1 v/v) and recrystallized from toluene/ethanol. Yield 1.39 g (39.6%), mp 240.0−241.0 °C. Found: C, 78.84%; H, 4.49%; N, 12.03%. Calcd: C, 79.45%; H, 4.60%; N, 11.99%. ^{1}H NMR ($CDCl_3$) δ 7.11−8.27 (m, 36H, aromatic H).

Synthesis of EM3: A mixture of 4-tetrazolyltriphenylamine (2, 3.14 g), *p*-phthaloyl chloride (1.10 g) and dry pyridine (90 mL) was stirred and heated under reflux for 57 h. After cooling, the mixture was poured into water, and the precipitate was collected and washed with water. After the mixture was cooled, the crude product was purified by column chromatography (developing solvent; chloroform:THF = 20:1 v/v) and

(39) Brown, H.; Kassal, R. *J. Org. Chem.* **1967**, *32*, 1871.
(40) Kadaba, P. K. *Synthesis* **1973**, 71.
(41) Abshire, C.; Marvel, C. *Makromol. Chem.* **1961**, *44−46*, 388.
(42) Huisgen, R.; Axen, C.; Seidl, H. *Chem. Ber.* **1965**, *98*, 2966.

recrystallized from toluene/ethanol. Yield 1.85 g (52.7%), mp 270.0–271.0 °C. Found: C, 79.13%; H, 4.64%; N, 11.92%. Calcd: C, 78.84%; H, 4.60%; N, 11.92%. ^{1}H NMR ($CDCl_3$) δ 7.11–8.27 (m, 36H, aromatic H).

Synthesis of EM4: A mixture of 4-tetrazolyltriphenylamine (2, 3.14 g), *o*-phthaloyl chloride (1.02 g) and dry pyridine (90 mL) was stirred and heated under reflux for 51 h. After cooling, the mixture was poured into water, and the precipitate was collected and washed with water. After the mixture was cooled, the crude product was purifled by column chromatography (developing solvent; chloroform:THF = 30:1 v/v) and recrystallized from toluene/*n*-Hex. Yield 0.70 g (20.0%), mp 217.0–218.0 °C. Found: C, 79.21%; H, 4.47%; N, 11.96%. Calcd: C, 78.84%; H, 4.60%; N, 11.92%. ^{1}H NMR ($CDCl_3$): δ 6.95–8.13 (m, 36H, aromatic H).

Synthesis of EM5: A mixture of 4-tetrazolyltriphenylamine (2, 3.14 g), 1,3,5-phthaloyl chloride (0.76 g) and dry pyridine (35 mL) was stirred and heated under reflux for 72 h. After cooling, the mixture was poured into water, and the precipitate was collected and washed with water. After the mixture was cooled, the crude product was purified by column chromatography (developing solvent; chloroform:THF = 30:1 v/v) and recrystallized from toluene/methanol. Yield 0.81 g (27.9%), mp 237.0–238.0 °C. Found: C, 78.55%; H, 4.40%; N,12.51%. Calcd: C, 78.32%; H, 4.48%; N, 12.45%. ^{1}H NMR ($CDCl_3$) δ 7.12–8.97 (m, 45H, aromatic H).

Hole-transport materials: We used six hole-transport materials, as shown in Figure 2. We synthesized these materials according to previous reports.[36,37,43] The HTM2 was synthesized via tris(4-iodophenyl)amine[44] with 3-methyldiphenylamine instead of the method of the previous report.[45]

Electron-transport and injection materials: We used 2,2′,2″-(1,3,5-benzenetriyl)tris[5-(1-naphthyl)-1,3,4-oxadiazole] (OXD3) and tris(8-quinolinolato)aluminum (Alq), as shown in Figure 1. We synthesized OXD3 via 1-naphthyltetrazole and trimesoyl chloride with high yield.[46] This ETM showed superior thermal stability in comparison with that of the PBD. Alq was purchased from Dojindo Laboratory.[47] We used Alq purified by vacuum sublimation.

2. **Fabrication of EL Devices**. Figure 3 shows the cell structures used in this study. Five types of EL cell structures were used to investigate the EL characteristics of emitter materials. The thickness of each organic layer is shown in Figure 3. In the triple hetero (TH) structure, we constructed a double electron-transport layer to lower the energy barrier to electron injection from a magnesium–silver (MgAg) cathode into the EML. Organic layers were deposited on a precleaned indium–tin oxide (ITO) glass substrate, and a cathode magnesium–silver (MgAg; 10:1 atomic ratio) layer was deposited on the organic layers by co-deposition in a 6×10^{-6} Torr vacuum at room temperature. Using a shadow mask, an active emission area of 2 × 2 mm was fabricated. The thickness of the ITO layer was 1700 Å, and the sheet resistance was about 20 Ω/□ (Asahi Glass Co., Ltd., sputtered film). The deposition rate for the organic layers was about 2 Å/s, and we could well control the thicknesses using a thickness monitor. Optical and scanning electron microscope observation revealed that every organic layer formed a uniform amorphous layer.

3. **Measurements of EL Characteristics**. After the fabrication of EL devices, we immediately measured the current–voltage–luminance (J–V–L) characteristics to eliminate the influence of environmental and storage conditions. The J–V–L measurements were performed from 0 V to the voltage at which the EL device underwent breakdown. Luminance was measured with a Topcon BM-7 luminance meter. Durability tests were done at a constant current density of J = 30 mA/cm^2. Here, we also immediately transferred the EL devices to a test tube as soon as possible after their fabrication. The atmosphere inside the test tube was replaced with N_2 gas three times and was kept under an overpressure of N_2 with fresh P_2O_5. Under this condition, we could suppress the growth of unavoidable small dark spots (nonemissive spots: ~5 μm) over a period of 1000 h. The initial fraction of dark spots in each EL device was less than 0.5%. The Ip values of the organic films were determined using a Riken-keiki AC-1. This analytical instrument is based on photoelectric effect. For detailed explanation, see the refs 48 and 49. The incident light intensity was fixed at 15 nW. Thermal analysis of emitter materials was done using a Rigaku TAS100. The rate of ascending temperature was maintained at 10 °C/min.

Table 1. Melting Point (T_m) and Glass Transition Temperature (T_g) of the Emitters (The Accuracy of the Measurements Was 0.1 °C

no.	T_m/°C	T_g/°C
EM1		133.6
EM2	270.0	122.3
EM3	234.3	118.2
EM4	218.2	99.3
EM5	238.7	166.5

Results and Discussion

1. Thermal and Optical Properties of Five Emitters. To obtain stable EL devices, increased thermal stability is an important factor, although apparently providing only high thermal stability to organic materials is not sufficient to obtain highly durable EL devices.[50] In EL devices, we mostly use the amorphous form of organic layers. Thus, we especially consider the stability of the amorphous state. Table 1 summarizes the melting point (T_m) and glass transition temperature (T_g) of five emitter materials. None of the materials showed a clear crystallization temperature (T_c), and we observed that these materials possessed high glass transition temperature over 99 °C, suggesting that they form desirable stable amorphous phases in a deposited film. The EM1, in particular, showed no clear T_m. It was really difficult to recrystallize the EM1 molecules with any conventional solvent on standing for over a month. Also, the starburst molecule, EM5, showed a pronounced increase in T_g (> 160 °C) and is expected to be a heat-stable material. The propeller structure of the three triphenylamine units possibly contributes to the desirable thermal properties. Also, in EM1, the hexafluoropropane linking unit is supposed to contribute to thermal properties effectively. Moreover, the comparison of EM2, EM3, and EM4 is also interesting. The bridging position of disubstituted phenylene greatly influenced their thermal properties, and the 1,4-disubstituted phenylene, EM2, showed the highest thermal stability among them.

Figure 4 summarizes photoluminescent (PL) and absorption spectra of the emitter thin films. Table 2 summarizes the peaks of the PL (PL(peak)) and the half-width of the half-intensity (hwhi) of emitter thin films. Absorption maxima and absorption edges are also summarized. These films were found to show strong photoluminescences (PLs) in the blue to blue-green region. A serious concentration quenching of PL in a thin-film form was not observed in these materials. The EM1 and EM3, in particular, showed strong blue PL. The insulating nature of the hexafluoropropane unit and

(43) Yamamoto, T.; Kurata, Y. *Can. J. Chem.* **1983**, *61*, 86.
(44) Kajigaeshi, S.; Kakinami, T.; Yamasaki, H.; Fujisaki, S.; Okamoto, T. *Bull. Chem. Soc. Jpn.* **1988**, *61*, 600.
(45) Shirota, Y.; Kobata, T.; Noma, N. *Chem Lett.* **1989**, 1145.
(46) Nagai, K.; Adachi, C.; Sakon, Y.; Tamoto, N. *Jpn. Kokai Tokkyo Koho*, JP93-280179.
(47) The Alq was purchased from Dojindo Laboratories, Kumamoto Techno Research Park, Japan.
(48) Kirihata, H.; Uda, M. *Rev. Sci. Instrum.* **1980**, *52*, 68.
(49) Riken Keiki Co. Ltd., Ozusawa 2-7-6, Itabashi-ku, Tokyo 174, Japan.
(50) Adachi, C.; Tamoto, N.; Nagai, K. *Appl. Phys. Lett.* **1995**, *66*, 2679.

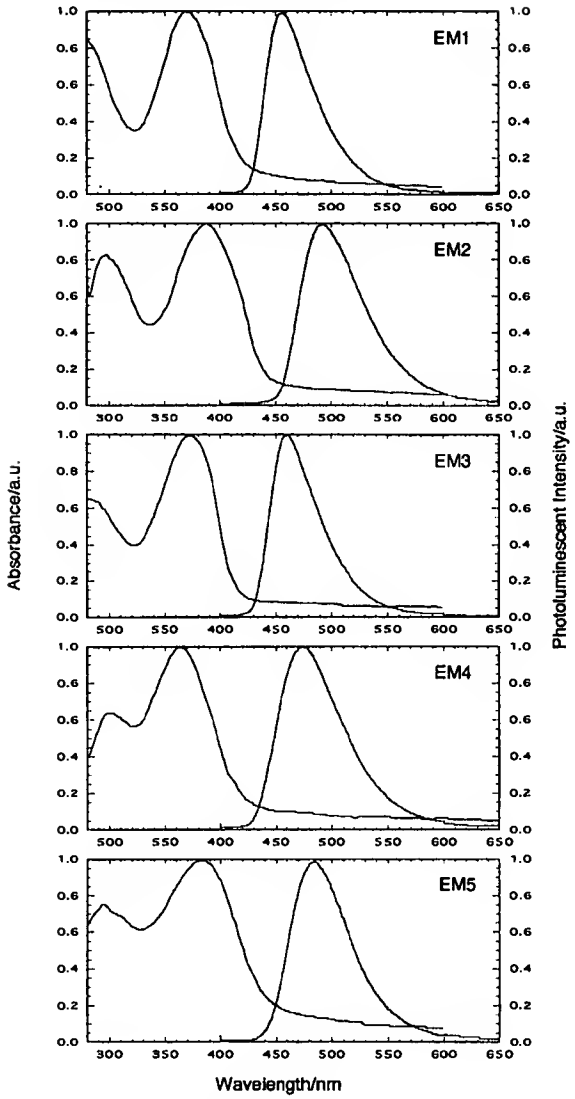

Figure 4. Absorption and photoluminescent spectra of deposited films of emitters (EM1-EM5). The absorbances and photoluminescent intensities are normalized.

Table 2. Photoluminescent (PL) and Absorption Characteristics of Emitter Thin Films (The Accuracy of the Measurements Was 0.1 nm)

no.	PL(peak)/nm	hwhi/nm	R.I./au	absorption max/nm	absorption edge/nm
EM1	454.4	64.5	23.3	368.8	417.0
EM2	489.4	73.5	13.3	386.6	437.0
EM3	458.4	62.9	35.5	371.0	412.3
EM4	469.0	74.8	15.9	362.8	415.8
EM5	487.2	85.0	1.2	382.0	439.0

the *m*-phenylene linkage contributes to the blue emission. On the other hand, because EM2 and EM4 are bonded to the p and o positions of phenylene, respectively, the extended π conjugation led to blue-green emission. Moreover, the comparison of EM5 with EM3 implies that the 1,3,5-trisubstitution slightly increases the π conjugation.

Table 3 summarizes the ionization potential (Ip)[51] and electron affinity (Ea)[51] of the emitter thin films. The

Table 3. Ionization Potential (Ip) and Electron Affinity (Ea) of Emitters (EM1–EM5), HTM (HTM1–HTM6), OXD3, and Alq Thin Films

no.	Ip/eV (HOMO)	Ea/eV (LUMO)
EM1	5.75	2.77
EM2	5.67	2.83
EM3	5.69	2.68
EM4	5.59	2.61
EM5	5.49	2.66
HTM1	5.08	2.10
HTM2	5.10	2.01
HTM3	5.39	2.28
HTM4	5.31	2.20
HTM5	5.49	2.33
HTM6	5.57	2.34
OXD3	5.93	2.69
Alq	5.70	3.00

Ea was estimated from the equation Ea = Ip − Eg; the Eg was determined tentatively from the edge of the absorption spectra.[52] The highest Ip value, 5.75 eV, was observed in EM1, suggesting an insulation effect of the linking unit of the hexafluoropropane group, while EM5 showed the lowest Ip value. In addition, Table 3 also summarizes the Ip and Ea of HTLs, OXD3, and Alq used in this study. Depending on the chemical structures of HTMs, a wide range of Ip values was observed. Later, we use these values for detailed discussion of the interaction between HTL/EML interfaces.

2. Electroluminescent Properties of Bipolar Emitters. Figure 5-1 shows the luminance–current characteristics of EL cells with five emitters in triple hetero (TH) structures. Here, we used HTM1 as an HTM. The EL devices with each emitter showed good EL performance over a wide range of a current density. In EM3, the maximum luminance of 6800 cd/m^2 was observed at a current density of 700 mA/cm^2. In contrast, the EL device with EM1 showed somewhat inferior characteristics in comparison with the other devices, although the PL intensity of the EM1 thin film is comparable to that of the other emitter layers.

Figure 5-2 shows the current density–voltage (J–V) characteristics of these EL cells. The EL device with EM3 exhibited the lowest resistivity, while the EL devices with EM2 and EM5 demonstrated higher resistivities. At J = 100 mA/cm^2, the difference in driving voltages reached 3.0V between EM3 and EM5. No close relationships between the Ip, Ea of EMs, and the driving voltages were observed. Thus, we assume that these differences should be ascribed to the delicate hole/electron carrier transport and injection characteristics of each EML.

Figure 6-1 shows the luminance–current (L–J) relationships of five EL devices. Here, we used HTM5 instead of HTM1 as an HTM. From the standpoint of increased ϕ_{EL}, the use of an HTM5 is particularly interesting, because we observed a pronounced increase in ϕ_{EL}. In EM2, for example, the ϕ_{EL} was increased by a factor of 3.44 in comparison with that with HTM1. The maximum luminance exceeded 10 000 cd/m^2 at a current density of J = 200 mA/cm^2. Furthermore, in Figure 6-2, the relationship between current–voltage (J–V) with HTM5 is interesting. The detailed com-

(51) Ionization potential (Ip) corresponds to the highest occupied molecular orbital (HOMO) and electron affinity (Ea) corresponds to the lowest unoccupied molecular orbital (LUMO).

(52) Electron affinity (Ea) of organic thin layers was provisionally determined by the method shown in the article by: Aminaka, E.; Tsutsui, T.; Saito, S. *Jpn. J. Appl. Phys.* **1994**, *33*, 4440.

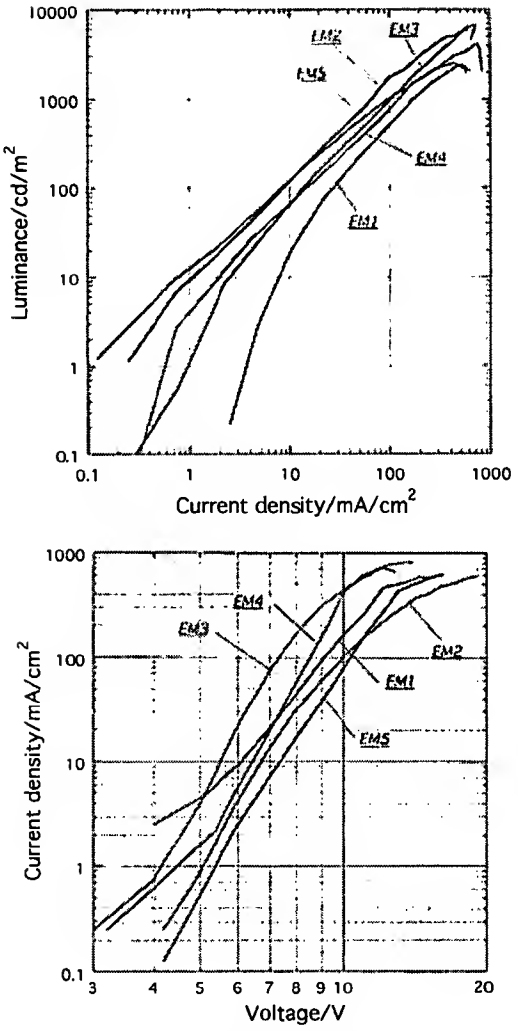

Figure 5. (5-1) Luminance–current density characteristics of five HTM1/emitter/ETL/EIL devices with emitters (EM1–EM5). (5-2) Current density–voltage characteristics of five HTM1/emitter/ETL/EIL devices with emitters (EM1-EM5).

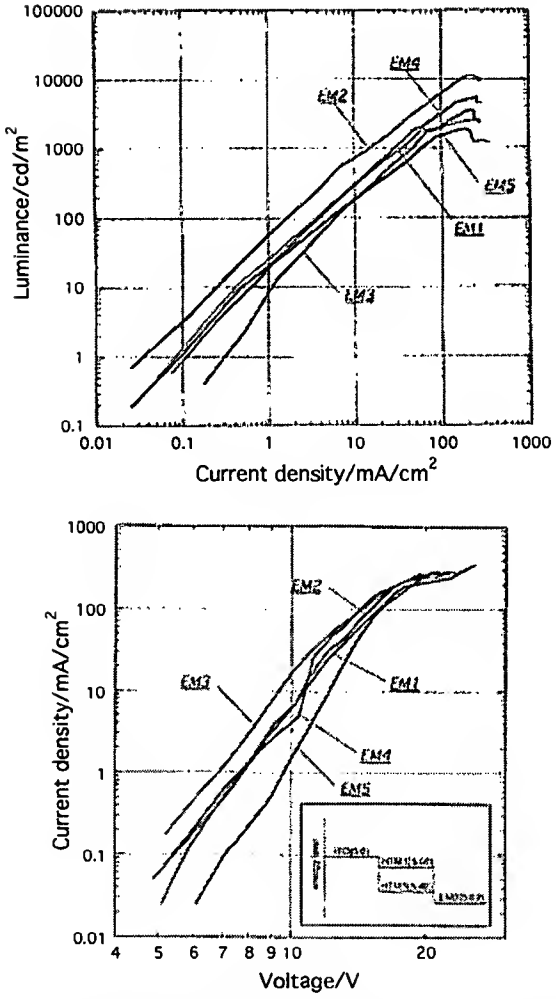

Figure 6. (6-1) Luminance–current density characteristics of five HTM5/emitter/ETL/EIL devices with emitters (EM1-EM5). (6-2) Current density–voltage characteristics of five HTM5/emitter/ETL/EIL devices with emitters (EM1-EM5).

parison of $J-V$ curves in Figures 5-2 and 6-2 showed that the resistivity of each EL device is appreciably enhanced with the use of HTM5. In EM3, a driving voltage increase of 3.9 V was observed at $J = 10$ mA/cm^2. The large energy barrier to hole injection at the interface of ITO/HTM5 directly influenced the increase in the driving voltage, considering the energy levels of the HTLs (Figure 6-2).

In addition, at a current density above 100 mA/cm^2, saturation behavior of the current flow was observed in each device. Due to the high resistivity of each EL device, it was really difficult to inject charge carriers exceeding 300 mA/cm^2.

3. Interactions between HTM and EM. The comparison of Figures 5 and 6 shows the importance of selecting HTMs for achieving a high ϕ_{EL}. Furthermore, we examined four other hole-transport materials as an HTL with the EM2 fixed as an emitter for a more detailed consideration of the interaction between HTL and EML. Figure 7 summarizes the luminance–current density ($L-J$) relationships with six HTMs. We recognize that the ϕ_{EL} was largely affected by the selection of the HTMs. Pronounced differences in the ϕ_{EL} were observed; a difference of about 1 order of

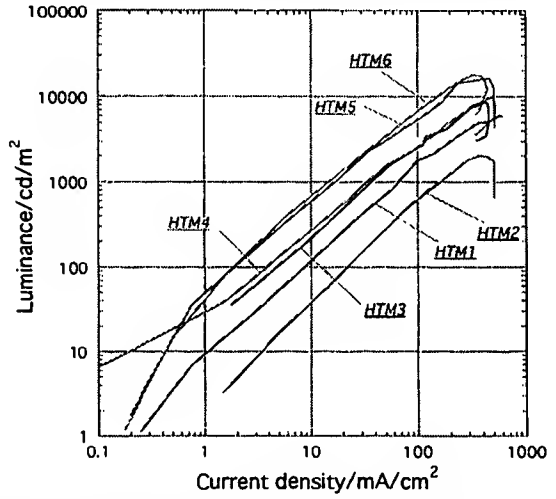

Figure 7. Luminance–current density characteristics of six HTM/EM2/ETL/EIL devices with (HTM1-HTM6).

magnitude was observed between HTM6 and HTM2. In the HTM6, the maximum luminance reached 19 000 cd/m^2, while the maximum luminance was only 2000 cd/m^2 in HTM2. In addition, the EL devices with HTM1, HTM3, and HTM4 showed intermediate emission ef-

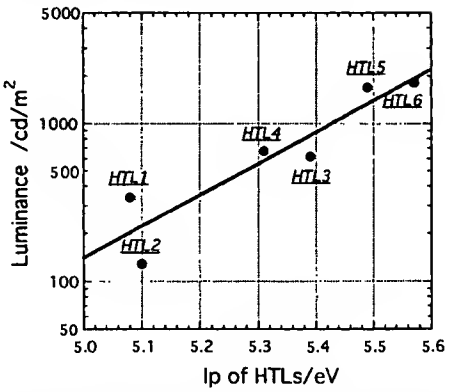

Figure 8. Relation between luminance at $J = 30$ mA/cm^2 and ionization potential (Ip) of hole-transport materials.

ficiencies. In HTM6, the ϕ_{EL} was estimated to be ~4%. This is one of the best values among previously reported EL devices without the use of a doping method.[53]

Additionally, we mention that luminance drops of over 400 mA/cm^2 are attributable to produced Joule heat, because several cells showed fusion and/or break of the EL devices at this current density. Also, the deviation from linear relationships of the $L-J$ curves below 1 mA/cm^2 should be ascribed to irregular and unavoidable pinholes in each EL device.

Figure 8 shows the relationships between the luminance at $J = 30$ mA/cm^2 and the Ip values of the HTLs. We observed an intimate relationship between them. The HTLs having a large Ip resulted in high ϕ_{EL} values, while the HTLs having a small Ip resulted in low ϕ_{EL} values. A comparison of the EL emission spectra of each EL device provides more information concerning the interaction between HTL and EML. To elucidate the interaction, we also prepared mixed thin films composed of HTMs and an EM2. Figures 9-1 and 9-2 summarize the EL spectra of six EL devices and the PL spectra of the mixed films, respectively. We observed a pronounced red-shift of the EL emission spectra in HTM1 and HTM2 which showed a low ϕ_{EL}, as shown in Figure 9-1. The broad EL spectrum with an hwhi of 100 nm was observed with HTM1. In HTM2, in particular, the appearance of a subpeak around 600 nm was observed. On the other hand, the EL spectrum of the device with HTM6 coincided well with the PL of EM2 and the hwhi was 75 nm, suggesting no exciplex formation. Additionally, in HTM3, HTM4, and HTM5, the EL spectra were slightly broadened. Their hwhi values were ~90 nm. Here, we compare these EL spectra with the PL spectra of the mixed films of HTMs and EM2, as shown in Figure 9-2. In the case of HTM1, we observed a drastic red-shift in the PL spectra in comparison with the dashed line showing the PL spectrum of the deposited EM2 film. The emission peak of the mixed film was around 532 nm, and the hwhi value was wide and reached 120 nm, while the PL spectrum of EM2 was centered at 489 nm with an hwhi of 74 nm. Furthermore, the mixed films of HTM3, HTM4, and HTM5 showed an appreciable shift in the PL spectra to the red of the EM2 spectra, while the HTM6 showed a slight blue-shift in the PL, suggesting no interaction between them. These red-shifts in the emission spectra with HTM1, HTM2, HTM3, HTM4, and HTM5 can be attributable to exciplex formation, because the absorption spectra of the mixed films of the HTM/EM2 showed superposition of each absorption spectrum and no extra absorption due to charge-transfer complexes were observed. For exciplex formation

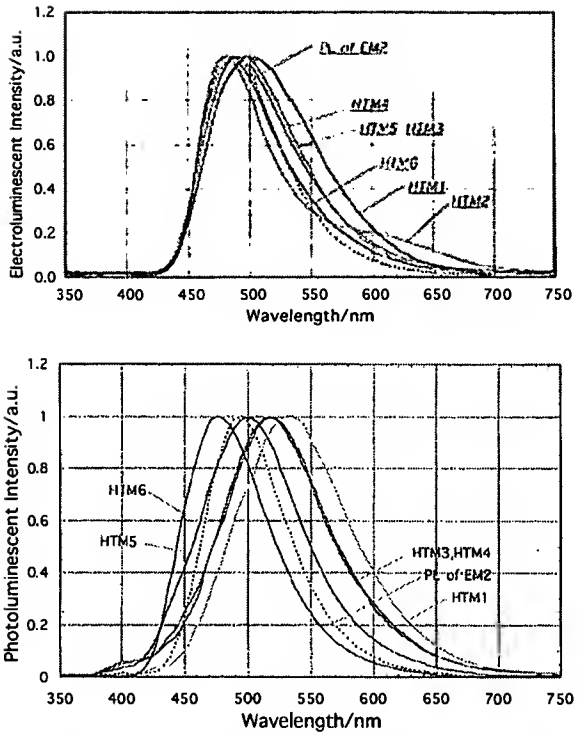

Figure 9. (9-1) EL emission spectra of five EL devices with HTM1-HTM5 and photoluminescent spectra of an EM2 thin film (dashed line). (9-2) Photoluminescent spectra of an EM2 thin film and five kinds of HTM/EM2 mixed films.

$$E_{max} = h\nu_{max} \propto Ip_{HTL} - Ea_{EML}$$[54,55]

where E_{max} refers to an emission maximum of the exciplexes. Ip_{HTL} is the ionization potential of HTLs; Ea_{EML} is the electron affinity of EMLs. Thus, for a constant EML, E_{max} will be proportional to Ip_{HTL}. Figure 10 shows the peaks of the PL wavelengths and the $Ip_{HTL} - Ea_{EML}$ relationships in HTL1, HTL3, HTL4, and HTL5. A nearly linear agreement was observed between them. This relationship and no corresponding change in the absorption spectra of the mixed films support the formation of exciplexes between the HTLs and the emitter layer. In addition, we observed different behavior in the mixed film of HTM2/EM2. It was really difficult to observe an intense PL from the mixed films. Because the HTM2 was a nonfluorescent material, the interaction between HTM2 and EM2 caused a predominant decay of the radiationless process. Although the origin of the subpeak around 600 nm which was observed in the EL spectrum is still not clear, we believe that the exciplex interaction of HTM2 and EM2 caused the emission. Furthermore, we mention the HTM6. The slightly blue-shift of the PL spectrum of the mixed film is possibly ascribed to the concentration effect of emitter molecules. We presume that the reduction of the interaction between emitter molecules

(53) Saito, S.; Tsutsui, T.; Era, M.; Takada, N.; Adachi, C.; Hamada, Y.; Wakimoto, T. *SPIE* **1993**, *1910*, 212.

(54) Turro, N. J. *Modern Molecular Photochemistry*; Benjamin/Cummings Publishing Co., Inc.: CA, 1978; Chapter 5.

(55) Weller, A. *Pure Appl. Chem.* **1968**, *115*, 16.

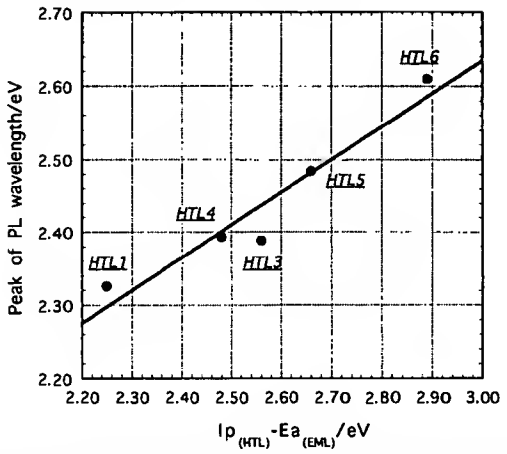

Figure 10. Relationships between peaks of photoluminescence and $Ip_{HTL} - Ea_{EML}$. Ip_{HTL}: ionization potential of HTL. Ea_{EML}: electron affinity of EML.

by the mixing of HTM6 molecules and also no interaction with HTM6 resulted in the blue-shift in the PL spectrum. Thus, the formation of exciplexes resulted in the red-shift of emitter layers and reduction of emission efficiency. As the Ip of HTLs became smaller, a lower EL intensity was observed, as shown in Figure 8. To obtain a high luminance, we should eliminate the formation of exciplexes. Thus, precaution should be exercised in selecting organic interfaces to achieve maximum efficiency of EL devices.

Here, additionally, we point out that the insertion of methyl groups into the structure of HTMs greatly influences the Ip values. In HTM5 and HTM6, the insertion of the 3,3′-dimethyl groups in biphenylylene caused twisting of the triphenylamine units and resulted in the high Ip value. Also, the insertion and positions of methyl groups into terminal phenyl groups played an important role in controlling the Ip values.

The observed EL spectra provide further information concerning emission sites inside an EML. The EL spectra are composed of the exciplex emission of the HTL/emitter interface and the emission of EMLs; therefore, the emission site is located near an interface of the HTL/emitter region. This means that the emitter layer, EM2, has an electron-transport tendency rather than a hole-transport tendency in a TH cell structure. Although triphenylamine units must have excellent hole-transport ability, the emitter serves as an electron transporter rather than a hole transporter. In fact, Tokuhisa et al. reported that this class of materials showed only hole mobility by the time-of-flight (TOF) method.[56] Thus, our results mean that carrier mobilities of emitter layers necessarily dominate carrier-transport properties. We should mention that carrier injection layers next to an emitter layer and the interface characteristic of organic layers play an important role in controlling the flow rates of hole and electron charge carriers.

4. Optimization of EL Cell Structures. The previous experimental results showed that carrier recombination sites lie near an HTL/EM interface. This means that we no longer need to construct TH and DH structures. We know that insertion of an ETL is assigned significance, when an EML has a hole-transport tendency and that an ETL plays an important role in confinement of charge carriers and molecular excitons. If an EML has an electron-transport tendency and accepts efficient electron injection from a cathode, an SH−A structure is already enough to obtain high EL performance. Thus, we again consider the optimum EL cell structures for obtaining high luminous efficiency. In this experiment, we used HTM6 as the HTL and EM2 as an emitter.

Figure 11-1 summarizes the $L-J$ characteristics in five kinds of EL cell structures. Because the emission site inside an EML was predicted to be near the interface of the EML/HTL, a remarkable difference in ϕ_{EL} between DH and TH structures was not observed. In contrast, the ϕ_{EL} of the SH−H was reduced to one-half that of the TH structure. Moreover, the construction of SL and SH−E structures resulted in a quite low ϕ_{EL} value. These results are consistent with the idea that the emitter layer has an electron-transport tendency rather than a hole-transport tendency. Because the emitter layer, EM2, has an electron-transport tendency, recombination sites are located near the interface of HTL/EML. Thus, almost the same emission efficiency was observed between TH and DH structures. However, in the SH−H structure, a decrease in ϕ_{EL} implies that the emission site probably moves toward the cathode side. Thus, we can recognize that the Alq electron injection layer (EIL) in the DH structure acts as a good electron injector from the cathode into an EML and contributes to the enhancement of ϕ_{EL}. Without the Alq layer, electron injection from the cathode into an EML is insufficient and resulted in an imbalance in the rate of hole/electron charge carriers. The energy barrier to electron injection at the cathode/EM2 interface influenced the balance of hole and electron current densities and caused a shift in emission sites. The DH structure is then adequate for the emitter, provided that the thickness of the emitter layer is over 15−20 nm to escape energy transfer into the Alq layer, because the emission sites are broadened by exciton migration and energy transfer to the Alq layer occurs.[57,58] In fact, when the thickness of the EML was less than 15 nm, we observed EL emission from both the emitter and the Alq layers.

Figure 11-2 shows the $J-V$ relationships of five EL devices. The TH and SH−E structures having an OXD3 layer showed rather high resistivity. We recognize that if emission sites are located near the HTL/EM interface, the insertion of the OXD3 layer is no longer necessary. Such layers resulted in high driving voltage and decreased ϕ_{energy}. On the other hand, the DH and SH−H structures showed lower resistivities. The DH structure, in particular, showed both lower resistivity and higher quantum efficiency. The luminous efficiency reached 3.75 lm/W at a current density of 10 mA/cm^2 with a driving voltage of 4.6 V and a luminance of 542 cd/m^2.

For obtaining excellent ϕ_{EL} values, we showed that an energetically appropriate combination of HTL and EML is required to eliminate exciplex formation. Furthermore, the formation of multi HTLs is expected to enhance both ϕ_{EL} and ϕ_{energy} values. The formation of

(56) Tokuhisa, H.; Era, M.; Tsutsui, T.; Saito, S. *Appl. Phys. Lett.* **1995**, *66*, 3433.

(57) Tang, C. W.; VanSlyke, S. A.; Chen, C. H. *J. Appl. Phys.* **1989**, *65*, 3610.

(58) Littman, J.; Martic, P. *J. Appl. Phys.* **1992**, *72*, 1957.

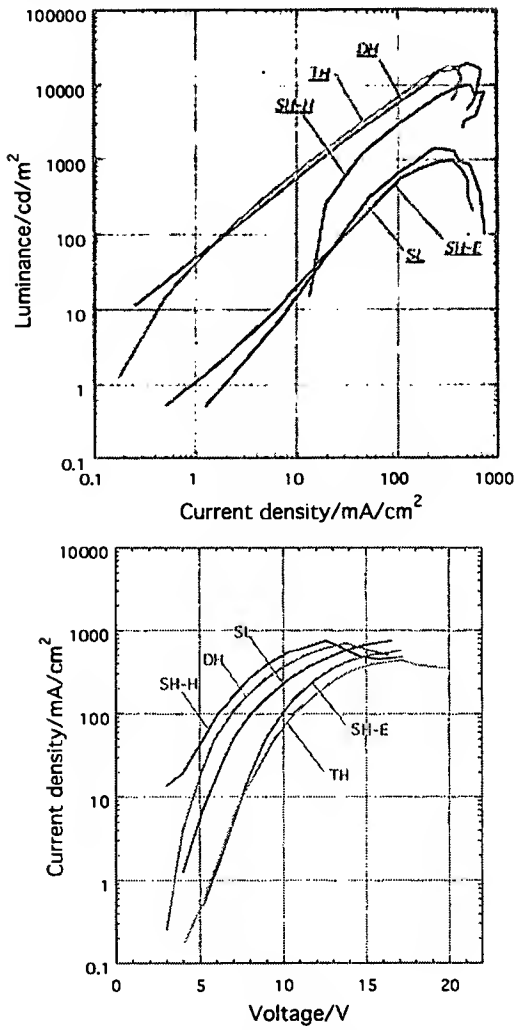

Figure 11. (11-1) Luminance–current density relationships of five kinds of EL devices: single layer (SL), single hetero-H (SH–H), single hetero-B (SH–E), double hetero (DH), and triple hetero (TH) structures. (11-2) Current density–voltage relationships with five kinds of EL devices: single layer (SL), single hetero-H (SH–H), single hetero-B (SH–E), double hetero (DH), and triple hetero (TH) structures.

an ITO/HTM2/HTM6/emitter/ETM/EIM structure surely provides the compatibility of ϕ_{EL} and ϕ_{energy}. We expect that the HTM2 will contribute to the reduction of the energy barrier for hole injection and that HTM6 will contribute to maintaining a high fluorescent yield of the emitter layers. Detailed experiments are now in progress.

5. Durability Characteristics of EL Devices. We measured the durability characteristics of EL devices at constant current density. Figure 12 shows the luminance change with time with five kinds of emitters in the cell structure of HTM5/emitter/ETM/EIM. The time in which the luminance decays to half the initial luminance was less than 1 h for each device. Also, rather rapid increases in driving voltages were observed with a drop in luminance, and the driving voltages of each device exceeded 20 V after 10 h continuous operation. In addition, we also examined the devices, HTM1/emitter/EIM, in which HTM1 was used instead of HTM5. Here, although a slight suppression of the increase in driving voltages was attained, we observed a small effect on suppression of the luminance drop. Moreover, our recent study revealed that when we use

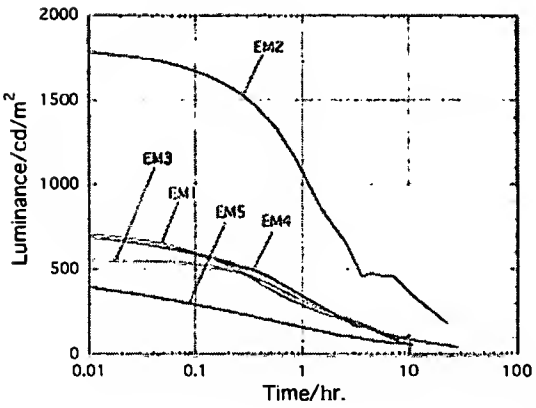

Figure 12. Time dependence of luminance at a constant current density of $J = 30$ mA/cm^2 in five EL devices.

aminopyrene dimer molecules instead of these emitters, the durabilities of the devices were remarkably enhanced in the same device configuration of a TH structure.[59] Thus, the primary short life of the devices with continuous dc operation is presumed to be attributable to the emitter materials. Because the thermal analysis revealed that these emitter materials showed excellent stability in the glassy state, another factor is presumed to govern device stability. Thus far, we experienced that EL materials possessing a flexible unit in their molecular structures resulted in inferior EL durability, although a distinct reason is still unclear. In our emitters, almost free rotation between the oxadiazole ring and the phenyl ring is allowed, because the five-membered oxadiazole ring is smaller than the phenyl ring. Thus, these classes of emitter molecules can be classified as low-durability materials. A detailed discussion will be published in a separate paper.[60]

Conclusions

We synthesized newly dimerized and trimerized molecules having an oxadiazole group as an electron-transport unit and a triphenylamine group as a hole-transport unit. We investigated the EL properties of these molecules as an emitter layer. The deposited films of all compounds were amorphous and showed strong blue-green fluorescence in the range 450–490 nm. In the EL process, we observed that EL quantum efficiency (ϕ_{EL}) was drastically influenced by the combination of hole-transport materials. Exciplex formation between an emitter and a hole-transport material was found to influence emission efficiency. We also studied optimum EL cell structures. With our best device, we achieved an energy efficiency of 3.75 lm/W at a current density of 10 mA/cm^2. The durabilities of EL devices were also measured at constant current density. The time in which the luminance decayed to half the initial luminance was only 1 h.

Acknowledgment. We acknowledge M. Sasaki, T. Shimada and M. Ohta for preparation of the organic materials and valuable discussions.

CM960391+

(59) Adachi, C.; Nagai, K.; Tamoto, N. *Jpn. J. Appl. Phys.* **1996**, *35*, 4819.
(60) Adachi, C.; Nagai, K.; Tamoto, N., manuscript in preparation.